A Study on Smoke Movement in Room Fires with Various Pool Fire Location

Jin-Yong Jeong, Hong-Sun Ryou*
Department of Mechanical Engineering, Chung-Ang University, 221 Huksuk-Dong, Dongjak-Ku, Seoul 156-756, Korea

In order to investigate the fire-induced smoke movement in a three-dimensional room with an open door, numerical and experimental study was performed. The center, wall, and corner fire plumes for various sized fires were studied experimentally in a rectangular pool fire using methanol as a fuel. The numerical results from a self-developed SMEP (Smoke Movement Estimating Program) field model were compared with experimental results obtained in this and from literature. Comparisons of SMEP and experimental results have shown reasonable agreement. As the fire strength became larger for the center fires, the air mass flow rate in the door, average hot layer temperature, flame angle and mean flame height were observed to increase but the doorway-neutral-planeheight and the steady-state time were observed to decrease. Also as the wall effect became larger in room fires, the hot layer temperature, mean flame height, doorway-neutral-planeheight and steady-state time were observed to increase. In the egress point of view considering the smoke filling time and the early spread of plume in the room space, the results of the center fire appeared to be more dangerous as compared with the wall and the corner fire. Thus it is necessary to consider the wall effect as an important factor in designing efficient fire protection systems.

Key Words : Smoke, Center, Wall, Corner, SMEP, Flame, Plume

1. Introduction

The control of smoke movement in room fires is often an important factor in designing efficient fire protection systems. The prevention of fires in rooms requires a good understanding and prediction of the temperature field and smoke concentration by the fire and the air flow through the door. Recent studies of fire plumes by Zukoski et al. (1981), and Quintiere et al. (1981), have shown that buoyant diffusion flames tend to entrain air more than an idealized point source plume, and that the smoke flow is influenced by fire strength and laboratory atmospheric disturbances. Yang (1994), Kerrison et al. (1994), and Ewer et al. (1999) studied several field models including PHOENICS, FLOW3D, SMARTFIRE and UNDSAFE and discussed the limitations and capabilities of the fire models. However, their studies have neglected the radiative heat transfer mechanisms and have focused on the comparison and evaluation of overall ability of the commercial CFD program. Consequently, what seems to be lacking in fire modeling is the effect of radiative heat transfer and suitable experimental benchmark fire data.

In field modeling, sub-models of combustion, turbulence and radiative heat transfer are needed to describe a fire phenomenon. One of the reasons why an enclosure fire is a complex phenomenon is that there are strong interactions among these

* Corresponding Author,
E-mail : cfdmec@cau.ac.kr
TEL : +82-2-820-5280; **FAX** : +82-2-813-3669
Department of Mechanical Engineering, Chung-Ang University, 221 Huksuk-Dong, Dongjak-Ku, Seoul 156-756, Korea. (Manuscript **Received** February 18, 2002; **Revised** July 2, 2002)

three effects. Xue et al. (2001) compared various combustion models in enclosure fire simulation. The difficulty of turbulent combustion model is due to the nature of enclosure fire phenomena where pyrolysis and gasification are inherent and very complex to model. Furthermore, it is not easy to accurately know the reaction kinetics and combustion rate in room fires. Radiation is an important heat transfer mode in fire modeling because of the high temperatures attained in rooms with fires or hot smoke layers. Predicting possible secondary ignition due to thermal radiation is particularly important in fire safety engineering, because it can prevent adjacent material from igniting. Hoffmann et al. (1988), Lockwood et al. (1989), Forney (1994), and Keramida et al. (1998) investigated the radiative heat transfer occurring in fire modeling and conducted intensive comparison and evaluation with fire experimental data. The isotropic scattering cases of radiative transfer in a two-dimensional rectangular room were studied by Fiveland (1984), using the S-N discrete ordinates method and by Thynell and Ozisik (1987), using the finite element method. In the present study, the physically controlled diffusion flame model (Spalding, 1971 and Bilger, 1975) including combustion based on the global single-step irreversible reaction was applied. Turbulence and radiation model used the modified k-epsilon turbulence model with buoyancy term and the S-N discrete ordinate method based on the weighed sum of gray gas model (Schmidt, 1982; Kim, 2001), respectively.

The smoke movement and flame structure produced by fires burning near a wall or a corner of a room is of great practical importance. Fire engineers are interested, for example, in the wall effect on the amount of smoke generated by fires, which is determined by the entrainment of ambient air into their plumes. They are also interested in the mean flame heights of fires burning near walls, which affect the spread of the fire. The subject has already received some attention (Grella and Faeth, 1975; Zukoski et al., 1981; Hasemi and Tokunaga, 1984; Hansell, 1993). However, the wall effect on typical accidental compartment fires is not fully understood. The general effect of walls on flame height can be explained qualitatively, but their exact quantitative effect is not known. Hansell (1993) has described the wall effect on the mass flux by the entrainment factor (EF). He then suggested that EF is equal to the ratio of the open or effective perimeter of the fuel source to its total perimeter. Accordingly, the values of EF for square fuel sources in the open, next to a wall and in a corner are 1, 0.75 and 0.5, respectively. Zukoski et al. (1981) conducted eopeniments to examine the effect of a vertical wall located close to a square fire source on the entrainment. Their measurements suggest that EF=0.57, which is considerably smaller than the value of 0.75 suggested by Hansell (1993) and slightly smaller than the value predicted by the Mirror Model. The Mirror Model (Hasemi and Tokunaga, 1984; Zukoski et al., 1981) assumes the existence of an imaginary fire source on the other side of the wall, which has the same intensity as the original fire source. Hasemi and Tokunaga (1984) measured the mean height of the continuous flame and the peak height of the flames direct by observation or by observation of its video recording. They have not measured the mass entrainment directly, but when the gas burner was placed at the corner of two walls, they showed that the peak and continuous flame heights were 23 and 67% higher than those in free standing burners. They have also measured the excess temperatures in the plume, which are inversely proportional to the entrainment of fresh air into the far-field plume, and have concluded that for both wall and corner fires, the actual temperature increase is considerably larger than that predicted by the Mirror Model.

The aim of the present study is to examine the wall effect on smoke movement and flame structure in three-dimensional room fires and to validate a self-developed SMEP field model. The results of the SMEP code using DOM radiation model and PISO algorithm were compared with the data obtained from the room fire experiments of Quintiere et al. (1981) and Steckler et al. (1982) and the experiments carried out in this study.

2. Experiments

The room dimensions were $1.8\times1.8\times1.38^{H}$m with a 1.18 m high by 0.48 m wide open door. The wall was made of about 10 mm thick acryl and asbestos slates. The experiments were conducted for three types of center, wall and corner fires by varying the fire strength (7.65, 21.25, 51.71 kW). Here the fire strength means the heat release rate of the fire source. Figure 1 shows the overall arrangement of measurement probes and room geometry. The fuel tray were made of 2 mm-thick steel plate and placed at the center of the floor (C in Fig. 1), at a wall (B in Fig. 1) and at the corner of two walls (A in Fig. 1). Different sizes of tray, 15×15 cm, 25×25 cm, 39×39 cm in surface area and 7 cm in depth, were used to vary the fuel surface area. Methanol (purity 99.9%) was used as the fuel. The mass burning rate of fuel was evaluated by measuring the weight of the fuel vessel continuously using the load cell. K-type thermocouples (measurement range: -270 ℃ ~ 1300 ℃) with a wire diameter of 0.32 mm were placed vertically in the center line of the open door and in the front corner of the room to measure the gas temperature profile.

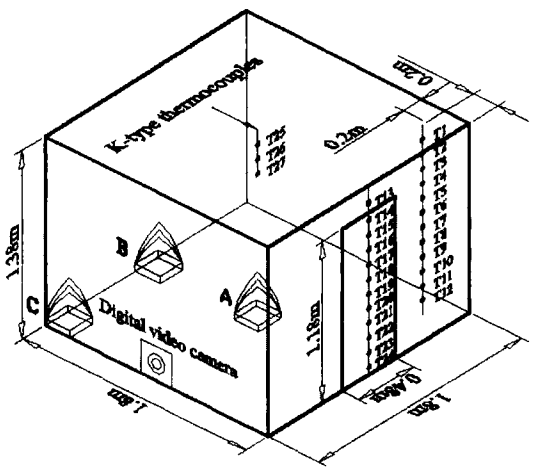

Fig. 1 Experimental arrangement and configuration

3. Mathematical Models

3.1 Flow field model

The flow is described by the three-dimensional, Favre-averaged equations of transport for mass, momentum, gas-species concentration and internal energy. Turbulence is modeled using the modified k-ε equation model which consides the production of turbulence due to buoyancy and the effect of thermal stratification of the turbulence dissipation rate. We consider a thermally expandable ideal gas driven by a prescribed heat source. The equations of motion governing the fluid flow are written in a form suitable for low Mach number applications. Sometimes, this form of the equations is referred to as "weakly compressible". The most important feature of these equations is that in the energy equation, the spatially and temporally varying pressure is replaced by an average pressure which depends only on time. Finite volume method and PISO algorithm are then employed for solving the linked set for velocity and pressure equations. The mathematical derivation are reported elsewhere (Issa, 1985; Peric, 1985) and will not be repeated here.

3.2 Combustion model

In the present numerical analysis, combustion products are discharged vertically upwards from the pool source placed in on floor. Gas present in the room becomes a mixture of air (O_2 and N_2), fuel and combustion products (H_2O and CO_2). The combustion model is based on the global single-step irreversible form

$$1\ kg\ fuel+s\ kg\ air \rightarrow (1+s)\ kg\ products \quad (1)$$

where s is the stoichiometric oxidant requirement of the fuel. To express the turbulent chemical source term in the species equation, it is often convenient to rewrite the equations in a form which does not contain any source term by introducing the mixture fraction f as a dependant variable (Gupta and Lilley, 1985; Xue, 2001). It is useful to describe the mixture field and to identify the location of the stochiometric mixture. The mixture fraction is defined from

$$f=\frac{\Phi-\Phi_\infty}{\Phi_F-\Phi_\infty},\ with\ \Phi=Y_{fu}-\frac{Y_{ox}}{s} \tag{2}$$

where Y_{fu} and Y_{ox} are the respective mass fractions of fuel and oxidant and the subscripts F and ∞ refer to fuel and oxidant streams for Φ, respectively.

The species conservation equations may then be written as

$$\frac{\partial}{\partial t}(\rho\bar{f})+\frac{\partial}{\partial x_j}(\rho u_j\bar{f})=\frac{\partial}{\partial x_j}\left(\frac{\mu_{eff}}{\sigma_f}\frac{\partial\bar{f}}{\partial x_j}\right)+S_f \tag{3}$$

where σ_f is the Prandtl/Schmidt number for (σ_f=0.7) and S_f is due solely to phase change. S_f=0, if there is no phase change.

The composition of the mixture is deduced from by f using the following relation

$$\begin{aligned}&\text{air excess}: 0\le f\le f_{sto}\Rightarrow Y_{ox}=Y_{ox,\infty}\frac{f_{sto}-f}{f_{sto}},\\ &\qquad Y_{fu}=0\\ &\text{fuel excess}: f_{sto}\le f\le 1\Rightarrow Y_{fu}=\frac{f-f_{sto}}{1-f_{sto}},\\ &\qquad Y_{ox}=0\\ &Y_{N2}=Y_{N2,\infty}(1-f)\\ &Y_{pr}=1-Y_{fu}-Y_{ox}-Y_{N2}\end{aligned} \tag{4}$$

where the stoichiometric value of f is $f_{sto}=[Y_{ox,\infty}/s]/[1+Y_{ox,\infty}/s]$.

3.3 Radiation model

Radiant energy lost by the plume significantly increases the temperature of the surrounding surfaces and modifies temperature and heat exchanges in the room. Radiation is produced by hot heteronuclear gas molecules and by soot particles. Soot production mechanisms are difficult to describe and depend on fuel nature and combustion conditions. We do not take account for the effects in the radiation model.

The S-N discrete ordinates method replaces the radiative transfer equation with a set of equations for a finite number of M ordinate directions (Chandrasekhar, 1960). To calculate the radiation equation in a three-dimensional space, the 8 sweep directions are considered as shown Fig. 2. The weighted diamond difference scheme is used in this study to relate the intensities in the control volume (Kim and Lee, 1988). The total emissivity which is equal to the absorption coefficient for a gray gas (Modest, 1991), is evaluated from the Weighted Sum of Gray Gases Model (WSGGM) proposed by Schmidt et al. (1982):

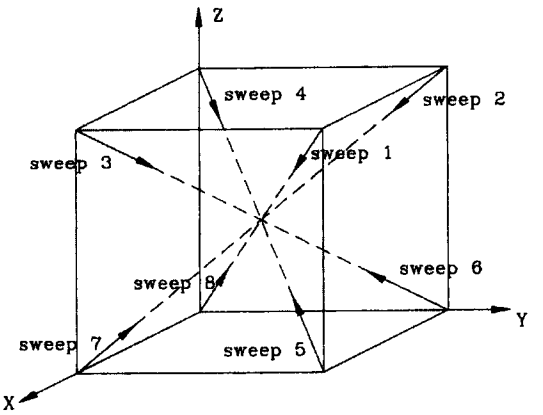

Fig. 2 Schematic diagram of the 8 sweep directions

$$\varepsilon=\sum_{i=0}^{I}a_{\varepsilon,i}(T)\left[1-\exp(-\kappa_i ps)\right] \tag{5}$$

where $a_{\varepsilon,i}$ which depend on the gas temperature T denote the emissivity weighting factors for the i-th gray gas. The bracketed quantity is the i-th gray gas emissivity with absorption coefficient, κ_i, and pressure-path length product, ps. For a gas mixture ps is the sum of the partial pressures of the absorbing gases. In the present analysis, three component gray gases are considered to represent the emissivity of the mixture (carbon dioxide, water vapor, and air). The expressions for the coefficients of the WSGGM are taken from the work of Schmidt et al. (1982).

4. Numerical Method

In the SMEP field model (Jeong et al., 2000), the difference schemes for discretizing the time term and the convection term into linear form used the Euler implicit scheme and the hybrid scheme, respectively. The computations were carried out on a Pentium III 600 personal computer. Figure 3 shows the grid generation of the room geometry. In order to correctly model the smoke movement in the doorway, the numerical grid was extended by 50 percent in length (x direction)

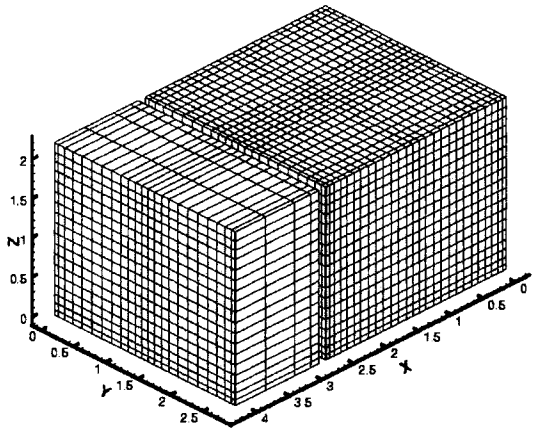

Fig. 3 Grid generation of the room geometry

including the region outside the fire compartment. A mesh of 13044 cells (11178 internal and 1866 external cells) in total was used to describe the geometry for comparison with the room fire experiments of Quintiere et al. (1981) and of Steckler et al. (1982). For the experiments carried out in this study, the computational grid used 10634 cells (9200 internal and 1434 external cells) for fire strength 7.65kW, 9014 cells (7728 internal and 1286 external cells) for fire strength 21.25kW and 13278 cells (11600 internal and 1678 external cells) for fire strength 51.71 kW, respectively. The mesh was non-uniformly distributed with refinements in the wall, floor, ceiling, fire and doorway regions. Within each time step, convergence was assumed if either the maximum number of iterations (100) was reached or the mass source residual fell to 1×10^{-3}. The time step used was 0.025s and experiments and simulations were performed up to ten minutes as this was considered sufficient time for smoke movement to arrive at the steady state. With regard to computing time, the computing time required was less than seven hours when the SMEP was executed on a Pentium III 600 PC.

4.1 Boundary and initial conditions

The initial temperature and pressure were set to be 293K (300K for the room fire experiments of Quintiere et al. (1981) and Stecker et al. (1982)) and 101,325 Pa. The insulating walls of the room were modeled with no-slip conditions for the velocities and adiabatic conditions for the temperature. A fixed pressure boundary condition was used on all external boundaries. Also the wall functions were used to bridge the near wall region. The wall boundary conditions for analysis of the radiative heat transfer are all gray and diffusely reflecting, and they may also be sources for thermal radiation. The wall intensities are written as

$$I_w(x, y, z, \Omega)=\varepsilon_w T_w^4(x, y, z) + \frac{1-\varepsilon_w}{\pi}\int_{\Omega'\vec{n}<0} |\Omega'\cdot\vec{n}|\, I_w(x, y, z, \Omega')\, d\Omega' \quad (6)$$

$$for\ \vec{n}\cdot\Omega>0$$

where $\vec{n}$ is the inward normal unit vector to the boundary wall and ε_w is the wall emissivity.

4.2 Plume model and inlet condition

The flame height depends on the fire geometry, the ambient conditions, the heat of combustion and the stoichiometric ratio. A relationship (Cox, 1995) for flame height that can be used for many fuels is

$$Z_{fl}=3.3Q_D^{*2/3}D_f \quad for\ Q_D^*<1 \quad (7)$$

$$Z_{fl}=3.3Q_D^{*2/5}D_f \quad for\ Q_D^*<1 \quad (8)$$

where, $Q_D^*=\dfrac{\dot{Q}}{\rho_\infty C_{p\infty}T_\infty(gD_f)^{1/2}D_f^2}$. In the equation, Z_{fl} is the mean flame height, $\dot{Q}$ in meters, is the heat release rate of the fire, in kW and D_f is the diameter of fire, in meters.

The virtual origin of the plume, ΔZ_f(m), (Heskestad, 1983) is

$$\Delta Z_f=1.02D_f-0.083\dot{Q}^{2/5} \quad (9)$$

The virtual origin can be above the top of the fuel or below the fuel. The sign convention is for the virtual origin above the top of the fuel ΔZ_f is negative, and for the virtual origin below the top of the fuel ΔZ_f is positive. The mass flow, $\dot{m}$(kg/s), of an axisymmetric plume at height Z_{fl} (Heskestad, 1984) is

$$\dot{m}=0.071\dot{Q}_c^{1/3}(Z_{fl}+\Delta Z_f)^{5/3}[1+0.026\dot{Q}_c^{2/3}(Z_{fl}+\Delta Z_f)^{-5/3}] \quad (10)$$

where $\dot{Q}_c$ is the convective heat release rate of fire, in kW.

Smoke was defined to include the air that is

entrained with the products of combustion. It follows that Eq. (9) can be thought of as an equation for the production of smoke from a fire. The average temperature of the plume can be obtained from a first law of thermodynamics analysis of the plume. For the steady plume the work is zero, and the changes in kinetic and potential energy are negligible. The first law leads to an equation for the plume temperature :

$$T_{zf}=T_{\infty}+\frac{\dot{Q}_c}{\dot{m}C_p} \tag{11}$$

where T_{zf} is the average plume temperature at elevation Z_{fl}, in K, T_{∞} is the ambient temperature, in K and C_p is the specific heat of plume gases, in kJ/kgK.

Fire plumes consist primarily of air mixed with the products of combustion, and the specific heat of plume gases is generally taken to be the same as air. The density of air and plume gases is calculated from the perfect gas law. The absolute pressure is taken to be standard atmospheric pressure of 101,325 Pa, and the gas constant is taken to be that of air which is 287 J/kgK.

The vertical upward speed v at height Z_{fl} above a fire for thermal plumes in free spaces can be expressed as

$$v=\frac{\dot{m}}{A\rho_{\infty}} \tag{12}$$

where v is in m/s, A is the fire source area in m^2 and ρ_2 is the density of ambient gas in kg/m^3.

The inlet boundary conditions of fire source can be specified using the temperature T_{zf} and velocity v obtained from the above equations.

5. Results and Discussion

In order to validate the self-developed SMEP code, the computation results were compared with data obtained from the room fire experiments of Quintiere (1981) and Steckler (1982). Figure 4 shows the experimental arrangements and configuration conducted by Quintiere (1981) and Steckler (1982). Here the fire source used the fire strength 62.9kW. Figure 5 shows the temperature distribution of SMEP, FLOW3D without radiation, and experimental data (Steckler et al., 1982) for doorway centerline temperature. A difference of more than 20 ℃ in the hot smoke layer is found between the temperature predicted by the commercial package FLOW3D without radiation effect and that obtained by the experiments of Steckler et al. (1982). On the other hand, the result of the SMEP with radiation effect has shown good agreement in comparison with the experimental data (Steckler et al., 1982). This is thought to be due to the radiation effect of H_2O and CO_2 gas under smoke productions. Consequently, it is shown that the radiation effect under smoke in fire should be specially considered in order to produce more realistic result.

The profiles of doorway centerline velocities

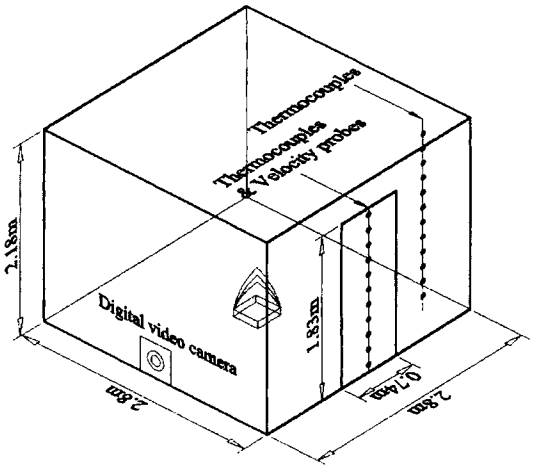

Fig. 4 Experimental arrangement and configuration (Quintiere et al., 1981 ; Steckler et al., 1982)

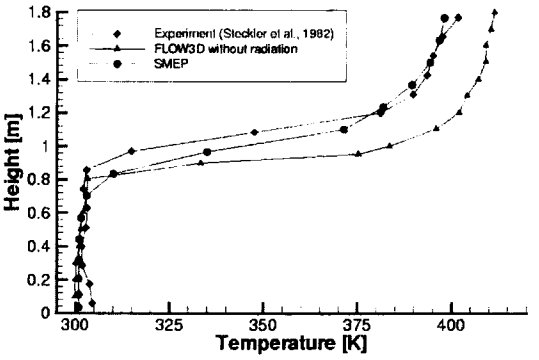

Fig. 5 Comparison of SMEP, FLOW3D and experiment (Steckler et al., 1982) for doorway centerline temperature

Table 1 Mass Flow Rate In/Out, Neutral Plane Height and Average Hot Layer Temperature produced by SMEP, FLOW3D without radiation and experiment (Steckler et al., 1982)

Classification	Mass Flow Rate In [kg/s]	Mass Flow Rate Out [kg/s]	Neutral Plane Height [m]	Ave. Hot Layer Temp. [K]
Steckler's Experiment	0.554	0.571	1.027	402
SMEP	0.575	0.588	0.92	399
FLOE3D Without radiation	0.582	0.591	0.926	407

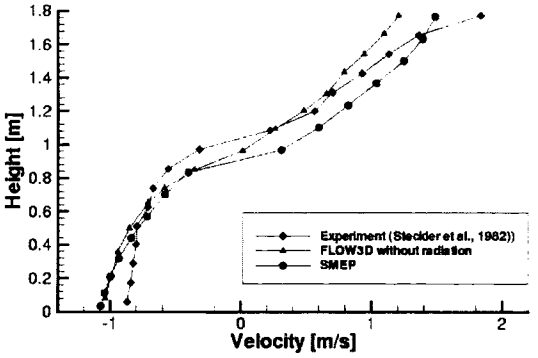

Fig. 6 Comparison of SMEP, FLOW3D and experiment (Steckler et al., 1982) for doorway centerline velocity

are depicted in Fig. 6 for the SMEP, the FLOW-3D, and experiment (Steckler et al., 1982). The numerical results of the two codes produce good agreement in comparison with experimental data (Steckleret al., 1982); However, they tend to underpredict velocities in the upper most portion of the door. Overall, the two numerical codes predict the measured values within about 10% error except the upper most portion of the door. In the upper most portion of the door (about 1. 8m high), the SMEP and FLOW3D underpredict about within 12% and 18% of the measured values respectively. This result was also reported in the SMARTFIRE and PHOENICS predictions by Ewer et al. (1999).

Table 1 shows the mass flow rates and neutral plane heights in the door and average upper layer temperature produced by SMEP, FLOW3D and experiment (Steckler et al., 1982). For the into and out mass flow rates through the door, the SMEP produces the discrepancy of 4% and 3%, respectively, with measured values, while the corresponding FLOW3D show the discrepancy of 5% and 4% respectively. For the neutral plane height, the two codes predict about within 11% in comparison with experimental result (Steckler et al., 1982). For the average upper layer temperature, the SMEP and FLOW3D predict about within 3% and 4% of the measured values. Similar results were also reported in the PHOENICS predictions by Kerrison et al. (1994).

Table 2 Comparison of SMPE and experiment (Quintiere et al., 1981) on the air mass flow rate for room with door (a) and window (b)

Opening configuration	Door [kg/s]	Window [Kg/s]
Experiment (Quintiere et al., 1981)	0.561	0.125
SMEP	0.5779	0.1133

Figure 7 shows the temperature distribution of SMEP and experimental data (Quintiere et al., 1981) in the corner for the room with a door and a window of the opening types. The window has the size of 0.46m hight by 0.74m width above 1.37m from floor. The results of the SMEP have shown reasonable agreement except in the lower layer region of Fig. 7(b) in comparison with the experimental data (Quintiere et al., 1981). Table 2 the air flow rates produced by SMEP with experimental results (Quintiere et al., 1981) for the room with a door and a window. For the air flow rates through the door and the window, there are discrepancies of 3% and 9%, respectively between what the SMEP roduces and the measured values. In conclusion, the results produced by SMEP showed reasonable agreement with experiment (Quintiere et al., 1981 ; Steckler

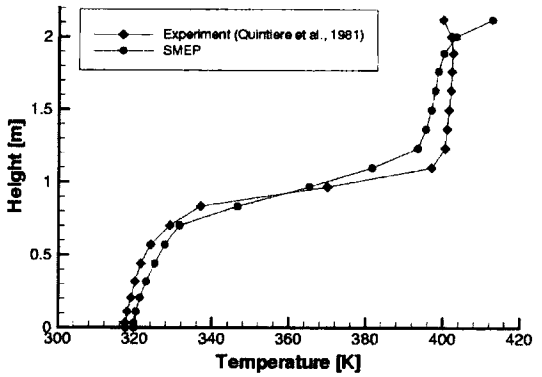

(a) For room with door

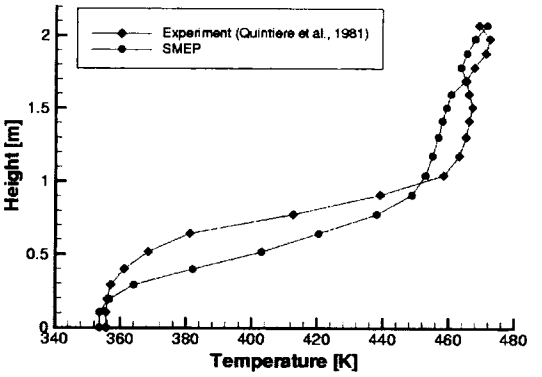

(b) For room with window

Fig. 7 Comparison of SMEP and experiment (Quintiere et al., 1981) on the vertical temperature distribution in the corner for room with door (a) and window (b)

et al., 1982) and perform better than those produced using commercial code FLOW3D.

Figure 8 depicts temperature contours and velocity vector through the center of the room as predicted by SMEP for the experiment of Quintiere et al. (1981). As can be seen from the figure, the degree to which the fire plume is deflected backwards by the induced incoming flow. While it is extremely difficult to make accurate measurements, the inclination of the SMEP (Fig. 8) produced plume appearing at approximately 50° to the horizontal. This result has shown about 7°~17° difference in comparison with the experimental observations-the (38±5)° to the horizontal-of Quintiere et al. (1981) in an earlier series of experiments. Figure 9 depicts the CO_2+H_2O mole fraction (a) and CO_2 mole fraction (b) contour through the center of the room as predicted

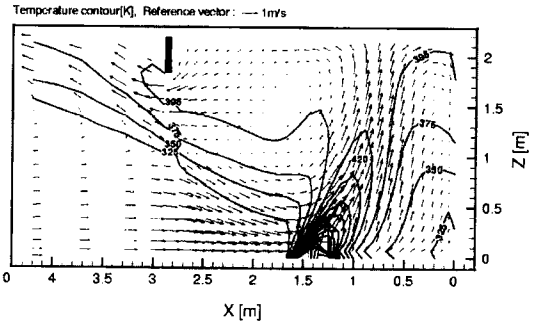

Fig. 8 Temperature contour and velocity vector through the center of the fire room passing through the doorway centerline predicted by SMEP for the experiment of Quintiere et al. (1981)

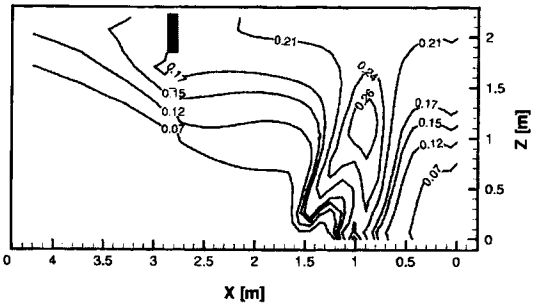

(a) CO_2+H_2O mole fraction [×100%]

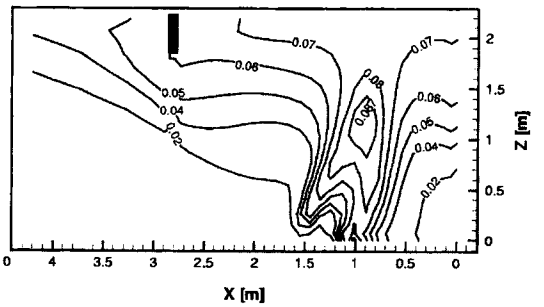

(b) CO_2 mole fraction [×100%]

Fig. 9 CO_2+H_2O mole fraction (a) and CO_2 mole fraction (b) contour through the center of the fire room passing through the doorway centerline predicted by SMEP for the experiment of Quintiere et al. (1981)

by SMEP. The CO_2+H_2O mole fraction and CO_2 mole fraction at the upper layer are about 21% and 7%, respectively. The CO_2+H_2O mole fraction and CO_2 mole fraction near the neutral plane height in the doorway centerline are about 7%

Table 3 Summary of SMEP and experimental results for center fire

Classification	Fire Strength, Q [kW]	Neutral Plane Height, N [m]	Mass Flux In, $\dot{m}_a$ [kg/s]	Flame/ Fire Plume Angle[°]	Ave. Hot Layer Temp. [K]
Experiment	7.65	0.66	0.141	63±5	331
SMEP	7.65	0.64	0.115	72	338
Experiment	21.25	0.64	0.188	55±5	367
SMEP	21.25	0.63	0.152	69	370
Experiment	51.71	0.60	0.243	45±5	428
SMEP	51.71	0.55	0.210	585	440

and 2%, respectively. This contour is similar to the temperature contour shown in Fig. 8.

Table 3 shows a summary of the SMEP computation and experiment performed in this work for center fires. All values obtained in the present study are measured after the steady state. Here the steady state was taken from the fire base to the stably stratified gas region in the room. The neutral plane height was determined from the thermal interface height deduced from the vertical temperature profile in the room. This height is determined by the position of rapid temperature change between the lower and upper portions of the room (Quintiere et al., 1981). Figure 10 shows the doorway centerline temperature of SMEP and experiment data for center fire. The comparison of SMEP and experiment has shown good agreement. In the third column of Table 3, the SMEP result of the neutral plane height predicts about within 8% of the measured values. The air flow rate through the door in the present experiment was estimated from the temperature data by the equation suggested by McCaffrey (1979). As the fire strength is increased from 7.65 kW to 51.71 kW, the air flow rate entrained through the door is observed to increase (see the fourth column of Table 3). Here the SMEP predicts the air mass flow rate to be within some 3% of the experimental results. This is to be expected as the air mass flow rate through the door is entrained by the density difference deduced from the large temperature difference in the doorway. As the fire strength becomes larger for the center fires, the inclination of the flame deflected backwards by the induced incoming flow is observed to increase. This seems to come

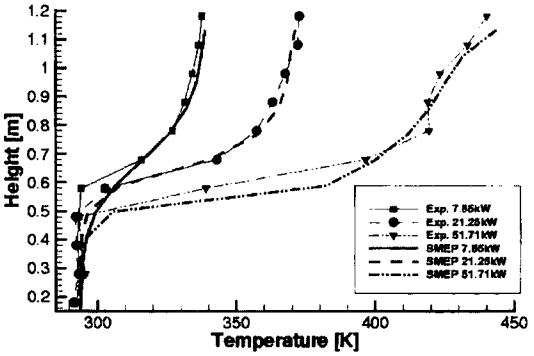

Fig. 10 Comparison of SMEP and experiment on the doorway centerline temperature for center fire

from the augmentation of the air entrainment rate through the door according to the increase of the heat release rate. Also the inclination of the fire plume obtained from the SMEP result has shown good agreement in comparison with the experimental observations (see the fifth column of Table 3). As the fire strength becomes larger, the average hot layer temperature is observed to increase. In the sixth column of Table 3, the SMEP predicts the average hot layer temperature to be within some 3% of the experimental results.

Figure 11 shows the comparison of doorway centerline temperatures between the SMEP and experimental data conducted by the authors for center, wall and corner fire with 21.25 kW. The comparison between numerical result and experimental data has produced reasonable agreement. Throughout the simulations, SMEP has tended to underestimate the location of the neutral plane. This accuracy is thought to be due to the mesh resolution within the doorway.

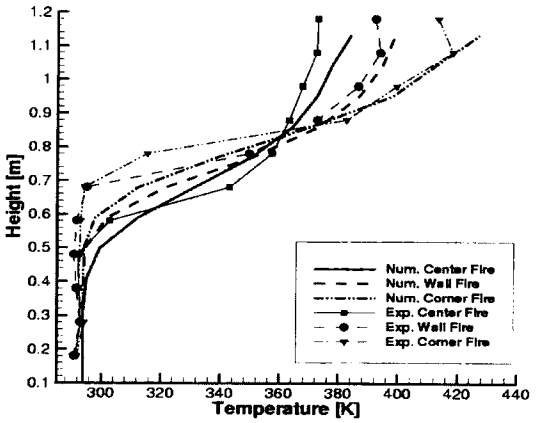

Fig. 11 Comparison of SMEP and experiment on the doorway centerline temperature for center, wall and corner fire with 21.25 kW

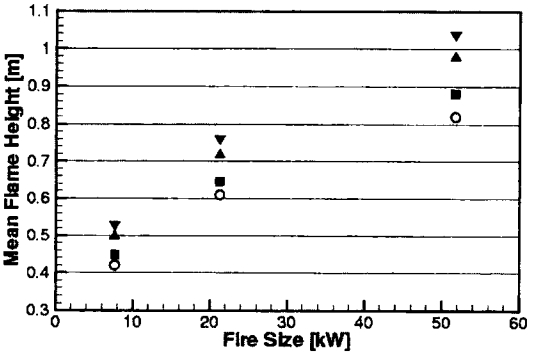

Fig. 12 Predicted and measured mean flame height as a function of fire strength for wall fires

Figure 12 shows the mean flame height as a function of fire strength for wall fires. As can be seen from the figure, the prediction obtained from the Hansell model (EF=0.75) provides a better description of the present measurements than those produced by the Zukoski (EF=0.57) and by the Mirror model (EF=0.63). Also for the corner fire, the Hansell model (EF=0.5) and the Mirror model (EF=0.4) predict about within 10% and 26% of the measured values, respectively.

Figures 13~15 show the temperature contour of SMEP for center, wall and corner fires with 21.25 kW. As can be seen from the figures, for the corner fire the hot layer temperature near the

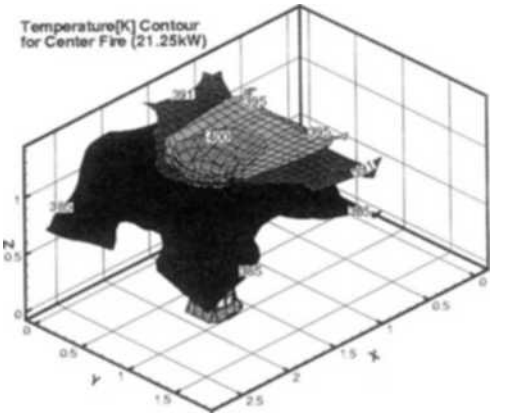

Fig. 13 Temperature contour of SMEP for center fire with 21.25 kW at 20 sec

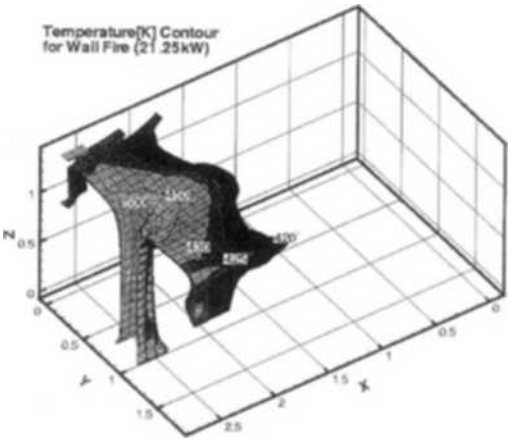

Fig. 14 Temperature contour of SMEP for wall fire with 21.25 kW at 17 sec

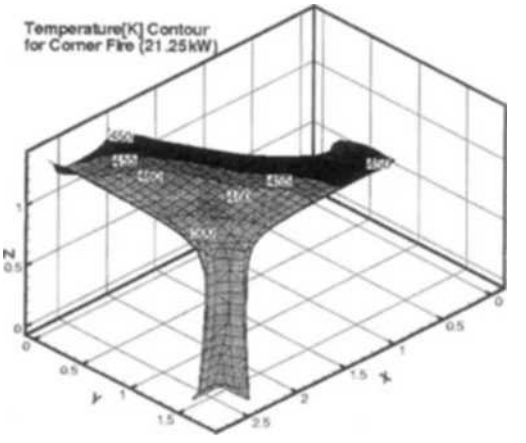

Fig. 15 Temperature contour of SMEP for corner fire with 21.25 kW at 19 sec

ceiling is higher than that produced by wall fire and center fire. However, for the smoke volume rate obtained by Mirror Model (Zukoski et al., 1981 ; Hasemi and Tokunaga, 1984) at the one-meter height from floor, the prediction of the center, wall and corner fire with the fire strength 21.25 kW is about 235885 cm^3/s, 135929 cm^3/s and 97726 cm^3/s, respectively. Thus, it is found that a corner fire has a very long time to fill the room space with smoke. In the egress point of view such as the smoke filling time and the early spread of flame and smoke in room space, the center fire is more dangerous as compared with the wall fire and corner fire.

6. Conclusions

To validate a self-developed SMEP field model, the SMEP results were compared with room fire experiment of Quintiere et al. (1981) and Steckler et al. (1982) and a commercial program (FLOW3D). The distributions of the temperature, velocity, air mass flow rate and neutral plane height in the doorway centerline predicted by SMEP have shown good agreement in comparison with experiments and FLOW3D results. Also, comparisons of SMEP and experiment in this work authors have shown reasonable agreement. The results of the calculated smoke temperature considering the radiation effect have shown good agreement compared with the experimental data. The radiation effect under smoke in fire should be specially considered in order to produce more realistic result.

As the fire strength became larger for the center fires, the air mass flow rate in the door, average hot layer temperature, flame angle and mean flame height were observed to increase but the doorway neutral plane height were observed to decrease. On the other hand, as the wall effect became larger in room fires, the hot layer temperature, mean flame height and doorway neutral plane height were observed to increase. For the corner fire the hot layer temperature near the ceiling was higher than that produced by wall fire and center fire. However, it was found that a corner fire has a very long time to fill the room space with smoke. In the egress point of view such as the smoke filling time and the early spread of plume in room space, the results of the center fire showed the more dangerous as compared with the wall and corner fire. Thus it is necessary to consider the wall effect as an important factor in designing efficient fire protection systems. The simple models for describing the effect of walls on the mean flame height were presented. The prediction obtained from the Hansell (1993) model provided a better description of the present measurements than those produced by the Zukoski et al. (1981) and by the Mirror Model.

Furthermore, in order to confirm the developed code, it is necessary to practice the extremely accurate experiment. Further work in various fire model validation is currently underway.

References

Bilger, R. W., 1975, "Turbulent Jet Diffusion Flames," *Progress in Energy and Combustion Sci.* Vol. 1, pp. 87~95.

Chandrasekhar, S., 1960, Radiative Transfer, Dover, New York, pp. 149~150.

Cox, G., 1995, Combustion Fundamentals of Fire, Academic Press, San Diego, CA, pp. 139~176.

Ewer, J., Galea, E. R., Patel, M. K., Taylor, S., Knight, B. and Petridis, M., 1999, "SMARTFIRE : An Intelegent CFD Based Fire Model," *J. of Fire Protection Engineering*, Vol. 10, No. 1, pp. 13~27.

Fiveland, W. A., 1984, "Discrete-Ordinates Solutions of the Radiative Transport Equation for Rectangular Enclosures," *ASME J. of Heat Transfer*, Vol. 106, pp. 699~706.

Forney, G. P., 1994, "Computing Radiative Heat Transfer Occurring in a Zone Fire Model," *Fire Sci. & Tech.*, Vol. 14, No. 1-2, pp. 31~47.

Gupta, A. K. and Lilley, D. G., 1985, Flow Field Modeling and Diagnostics, Abacus Press, Kent, U. K.

Hansell, G. O., 1994, Heat and Mass Transfer Process Affecting Smoke Control in Atrium Building, Ph. D. Thesis, South Bank Univ., London.

Heskestad, G., 1983, "Virtual Origins of Fire Plumes," *Fire Safety J.*, Vol. 5, No. 2, pp. 109~114.

Heskestad, G., 1984, "Engineering Relations for Fire Plumes," 여Fire Safety J., Vol. 7, No. 1, pp. 25~32.

Hoffmann, N. and Markatos, N. C., 1988, "Thermal Radiation Effects on Fire Enclosures," *Applied Mathematical Modelling*, Vol. 12, pp. 129~139.

Issa, R. I., 1985, "Solution of the Implict Discretised Fluid Flow Equations by Operator-Spliting," *Journal of Computational Physics*, Vol. 62, No. 1, pp. 40~65.

Jeong, J. Y., Ryou, H. S., Kim, S. C. and Kim, C. I., 2000, "A Numerical Study of Smoke Movement in Atrium Fires with Ceiling Heat Flux," *Proc. of the Fourth Asia-Oceania Sym. on Fire Sci. and Tech.*, pp. 425~437.

Keramida, E. P., Karayannis, A. N., Boudouvis, A. G. and Markatos, N. C., 1998, Radiative Heat Transfer in Fire Modeling, National Institute of Standards and Technology, NISTIR 6242.

Kerrison, L., Mawhinney, N., Galea, E. R., Hoffmann, N. and Pate, M. K., 1994, "A Comparison of Two Fire Field Models with Experimental Room Fire Data," *Fire Safety Science-Proc. of the Fourth Int. Sym.*, pp. 161~172.

Kim, T. K. and Lee, H. O., 1988, "Effect of Anisotropic Scattering on Radiative Heat Transfer in Two-Dimensional Rectangular Enclosures," *Int. J. of Heat Mass Transfer*. Vol. 31, No. 8, pp. 1711~1721.

Kim, T. K., Park, W. H. and Lee, C. H., 2001, "Radiative Transfer Solutions for Purely Absorbing Gray and Nongray Gases Within a Cubical Enclosure," *KSME Int. J.*, Vol. 15, No. 6, pp. 752~763.

Lockwood, F. C. and Shah, N. G., 1989, "A New Radiation Solution Method for Incorporation in General Combustion Prediction Procedures," *Eighteenth Symposium (international) on Combustion*, London, 1405.

McCaffery, B. J., 1979, Purely Buoyant Diffusion Flames: Some Experimental Results, National Bureau of Standards, NBSIR 79-1910.

Modest, M. F., 1991, "The Weighted Sum of Gray Gases Model for Arbitrary Solution Methods in Radiative Transfer. *J. of Heat Transfer*," Vol. 113, pp. 650~656.

Peric, M., 1985, A Finite Volume Method for the Prediction of Three Dimensional Fluid Flow in Complex Ducts. Ph. D, Imperial College.

Quintiere, J. G., Rinkinen, W. J. and Jones, W. W., 1981, "The Effect of Room Openings on Fire Plume Entrainment," *Combustion Science and Technology*, Vol. 26, pp. 193~201.

Schmidt, T. F., Shen, Z. F. and Friedman, J. N., 1982, "Evaluation of Coefficients for the Weighted Sum of Gray Gas Model," *J. of Heat Transfer*. Vol. 104, pp. 602~608.

Spalding, D. B., 1971, "Concentration Fluctuation In a Rount Free Jet," *Chem. Eng. Sci.*, Vol. 26, pp. 95~103.

Steckler, K. D., Quintiere, J. G. and Rinkinen, W. J., 1982, Flow induced by Fire in a Compartment. NBSIR 822520, National Bureau of Standards, Washington, DC.

Thynell, S. T. and Ozisik, M. N., 1987, "Radiation Transfer in Isotropically Scattering Rectangular Enclosures," *J. of Thermophys*, Vol. 1, No. 1, pp. 69~76.

Xue, H., Ho, J. C. and Cheng, Y. M., 2001, "Comparison of Different Combustion Models in Enclosure Fire Simulation," *Fire Safety J.*, Vol. 36, pp. 37~54.

Yang, K. T., 1994, "Recent Development in Field Modeling of Compartment Fires," *JSME Int. J Ser. B* Vol. 37, No. 4, pp. 702~717.

Zukoski, E. E., Kubota, T. and Cetegen, B., 1981, "Entrainment in Fire Plumes," Fire Safety J., Vol. 3, pp. 107~121.